

This article was downloaded by: [Xian Jiaotong University]

On: 11 December 2014, At: 13:23

Publisher: Taylor & Francis

Informa Ltd Registered in England and Wales Registered Number: 1072954 Registered office: Mortimer House, 37-41 Mortimer Street, London W1T 3JH, UK



## Molecular Crystals and Liquid Crystals

Publication details, including instructions for authors and subscription information:

<http://www.tandfonline.com/loi/gmcl20>

### Synthesis and Phase Structures of Dendronized Polymers with Dendritic Azobenzene Side Groups Based on Mesogen-Jacketed Liquid Crystalline Polymers

Chang-an Yang<sup>a</sup>, Ying Lu<sup>a</sup>, Gangyong Li<sup>a</sup> & Zhoubing Huang<sup>a</sup>

<sup>a</sup> Department of Chemistry and Chemical Engineering, Hunan Institute of Science and Technology, Yueyang, Hunan Province, P. R. China

Published online: 28 Apr 2014.

To cite this article: Chang-an Yang, Ying Lu, Gangyong Li & Zhoubing Huang (2014) Synthesis and Phase Structures of Dendronized Polymers with Dendritic Azobenzene Side Groups Based on Mesogen-Jacketed Liquid Crystalline Polymers, *Molecular Crystals and Liquid Crystals*, 592:1, 28-43, DOI: [10.1080/15421406.2013.837996](https://doi.org/10.1080/15421406.2013.837996)

To link to this article: <http://dx.doi.org/10.1080/15421406.2013.837996>

PLEASE SCROLL DOWN FOR ARTICLE

Taylor & Francis makes every effort to ensure the accuracy of all the information (the "Content") contained in the publications on our platform. However, Taylor & Francis, our agents, and our licensors make no representations or warranties whatsoever as to the accuracy, completeness, or suitability for any purpose of the Content. Any opinions and views expressed in this publication are the opinions and views of the authors, and are not the views of or endorsed by Taylor & Francis. The accuracy of the Content should not be relied upon and should be independently verified with primary sources of information. Taylor and Francis shall not be liable for any losses, actions, claims, proceedings, demands, costs, expenses, damages, and other liabilities whatsoever or howsoever caused arising directly or indirectly in connection with, in relation to or arising out of the use of the Content.

This article may be used for research, teaching, and private study purposes. Any substantial or systematic reproduction, redistribution, reselling, loan, sub-licensing, systematic supply, or distribution in any form to anyone is expressly forbidden. Terms &



# Synthesis and Phase Structures of Dendronized Polymers with Dendritic Azobenzene Side Groups Based on Mesogen-Jacketed Liquid Crystalline Polymers

CHANG-AN YANG,\* YING LU, GANGYONG LI,  
AND ZHOUBING HUANG

Department of Chemistry and Chemical Engineering, Hunan Institute of Science and Technology, Yueyang, Hunan Province, P. R. China

*The first- and second-generation dendronized polymers, poly (2, 5-bis {[3, 5-di (4'-methoxy-4-oxihexyloxy azobenzene) benzyl] oxycarbonyl} styrene) (PG1) and poly (2, 5-bis {[3, 5-di [3, 5-di (4'-methoxy-4-oxihexyloxy azobenzene) benzyl] oxycarbonyl} styrene) (PG2), were successfully synthesized, and their phase structures were investigated by differential scanning calorimetry (DSC), polarized light microscopy (PLM), and one-dimensional wide-angle X-ray diffraction (1D WAXD). The results show that the liquid crystalline (LC) phase structures of the dendronized polymers containing dendritic azobenzene side groups depend strongly on the molecular weights (MWs) and the generation of dendritic azobenzene side groups. Compared the low MWs PG2 with the low MWs PG1, the degree of order in LC phase increased with increasing the generation of dendritic azobenzene side groups.*

**Keywords** Dendritic azobenzene group; dendronized polymer; liquid crystals; phase structure

## 1. Introduction

Dendronized polymers have attracted much attention in the last decades because of their unique structure, properties, and potential applications in the field of catalyst support, electrooptic materials, and biological mimic, and so forth [1–3]. Dendronized polymers are a special class of nanoscopic molecules with a linear main-chain and pendant dendrons side groups at each repeating unit, which may adopt an extended and/or rod-like conformation due to steric congestion. For the dendronized polymers, it can be synthesized via different strategies including macromonomer route, graft-to route, and graft-from route [4–8].

Over the last 20 years, various dendronized polymers were synthesized and reported by Fréchet [1,2,8], Tomalia [9], Schlüter [4–6,10,11], Percec [3,12–20], Xi, and Chen

---

\*Address correspondence to Chang-An Yang, Department of Chemistry and Chemical Engineering, Hunan Institute of Science and Technology, Yueyang 414006, Hunan Province, P. R. China. Tel: +86-730-8640122; Fax: +86-730-8640122. E-mail: Chang\_anyang@163.com

[21–23]. The research showed that the phase behaviors and associated material properties of dendronized polymers were influenced by many various parameters, such as the type of dendron, the length of the tail of dendron, the generation of dendron, and so on. Dendronized polymers with Fréchet-type benzyl ether dendrons could not form extended and stiff conformation and are amorphous [2,8]. However, dendronized polymers containing Percec-type dendron side groups could form cylindrical conformation due to the spatial requirement of bulky dendrons, which develop cub phase, hexagonal columnar ( $\Phi_H$ ) phase, columnar nematic ( $\Phi_N$ ), tetragonal phase, and so on [12–20]. Schlüter-type ionic dendronized polymers also could self-assemble into hexagonal columnar ( $\Phi_H$ ) phase, columnar nematic ( $\Phi_N$ ), tetragonal phase, and rectangular phase [4,5,11]. In addition, the effects of the generation and length of the tail of dendron on the chain conformation and phase behaviors of dendronized polymer have been investigated by Mezzenga [5]. For the first-generation dendronized polymers with short-tailed lipid, the polymer showed an amorphous structure. By increasing the length of the lipid tail, lamellar phase could be observed. When the length of the lipid tail of dendrons was kept at fixed length, the first-generation dendronized polymer only formed a lamellar phase because of the small steric hindrance, similarly as linear polymer lipid complexes. With increasing generation, however, the main-chain was forced to take an extended and stiff conformation because of the steric hindrance between the bulky dendrons, leading to a columnar tetragonal phase rather than a lamellar phase. Moreover, the chain conformation of polymers also plays an important role in controlling their phase behaviors and associated material properties. Percec reported a general strategy for the rational control of polymer conformation through the self-assembly of quasi-equivalent monodendritic side groups attached to flexible backbones. At low molecular weights (MWs), the conical monodendrons assembled to produce a spherical polymer with random-coil backbone conformation. On increasing the MWs, the self-assembly pattern of the monodendritic units changed to give cylindrical polymers with extended backbones [14]. Recently, the dendronized polymers with different end-functional groups have also been reported, and their properties could be induced by changing the end-functional groups. Most of works concentrate on the effect of the type of the end-functional groups (e.g., flexible alkyl, amine, hydroxyl, and ionic mesogens) and on their material properties [4,5,24,25]. However, few works have been done on the synthesis of dendronized polymer with dendritic azobenzene side groups.

Mesogen-jacketed liquid crystalline polymers (MJLCPs) are a special class of side-chain liquid crystalline polymers (SCLCPs) in which the mesogenic units are laterally attached to the polymer backbone without or with very short spacers [26]. The steric hindrance produced by the bulky and rigid side groups will force the main-chain to exhibit an extended and stiff conformation similar to dendronized polymers [4,5,11–20]. In the past two decades, systematic research on the structure–property relationships for MJLCPs with different side groups has been done [27–33]. Recently, the functionalization of this system has been researched. The first- and second-generation dendronized carbazoles were introduced by the “graft through” method into MJLCPs for the first time [34]. The phase structures and optoelectronic properties of the resulting polymers were investigated. The results were shown that the first-generation polymer formed a hexatic columnar nematic phase, while the second-generation one exhibited a columnar nematic phase. This stiff main-chain conformation and the dendritic side group structure could reduce the intramolecular interactions and aggregations of the carbazole side groups and prevent the formation of excimers, which would be beneficial to the optoelectronic properties. Azobenzene mesogen is one of the typical functional units, which can undergo photon-driven reversible *cis–trans*

Downloaded by [Xian Jiaotong University] at 13:23 11 December 2014

Downloaded by [Xian Jiaotong University] at 13:23 11 December 2014

## Downloaded by [Xian Jiaotong University] at 13:23 11 December 2014

## Downloaded by [Xian Jiaotong University] at 13:23 11 December 2014

Downloaded by [Xian Jiaotong University] at 13:23 11 December 2014



Downloaded by [Xian Jiaotong University] at 13:23 11 December 2014

Chlorobenzene was washed with  $\text{H}_2\text{SO}_4$ ,  $\text{NaHCO}_3$ , and distilled water separately and was distilled from calcium hydride. Tetrahydrofuran (THF, AR; Beijing Chemical Co., China) and triethylamine (Acros, 99%; J&K Scientific Ltd., China) were heated under reflux over calcium hydride for at least 8 hr and distilled before use. All other reagents were used as received from commercial sources.

## 2.2. Measurements

Elemental analysis was carried out with an Elementar Vario EL instrument.  $^1\text{H}$  NMR spectra were recorded on a Bruker ARX400 spectrometer at room temperature, using deuterated chloroform ( $\text{CDCl}_3$ ) as the solvent and tetramethylsilane (TMS) as the internal standard.

The apparent number-average MW ( $M_n$ ) and MW distribution ( $M_w/M_n$ ) were measured on a GPC (Waters 1515) instrument with a set of HT3, HT4, and HT5. The  $\mu$ -Styragel columns used THF as an eluent, and its flow rate was  $1.0 \text{ mL min}^{-1}$  at  $35^\circ\text{C}$ . Calibration was made with polystyrene standards (PS).

The thermogravimetric analysis (TGA) was performed on a TA SDT 2960 instrument at a heating rate of  $20^\circ\text{C min}^{-1}$  in nitrogen atmosphere.

DSC examination was carried out on a TA DSC Q100 calorimeter with a programmed heating procedure in nitrogen. The sample size was about 5 mg and encapsulated in hermetically sealed aluminum pans, whose weights were kept constant. The temperature and heat flow scale at different cooling and heating rates were calibrated using standard materials such as indium and benzoic acid.

LC texture of the polymers was examined under PLM (Leica DM-LM-P) coupled with a Mettler-Toledo hot stage (FP82HT). The films with thickness of  $\sim 10 \mu\text{m}$  were casted from THF solution and slowly dried at room temperature.

1D WAXD experiments were performed on a Philips X' Pert Pro diffractometer with a 3 kW ceramic tube as the X-ray source ( $\text{Cu K}\alpha$ ) and an X' celerator detector. The reflection peak positions were calibrated with silicon powder ( $2\theta > 15^\circ$ ) and silver behenate ( $2\theta < 10^\circ$ ). The sample stage is set horizontally, and a temperature control unit (Paar Physica TCU 100) in conjunction with the diffractometer was utilized to study the structure evolutions as a function of temperature. The heating and cooling rates in the WAXD experiments were  $10^\circ\text{C min}^{-1}$ .

## 2.3. Synthesis of Monomers

The synthetic route of the monomers, 2, 5-bis {[3, 5-di (4'-methoxy-4-oxyhexyloxy azobenzene) benzyl] oxycarbonyl} styrene (denoted as G1) and 2, 5-bis {[3, 5-di [3, 5-di (4'-methoxy-4-oxyhexyloxy azobenzene) benzyl] oxycarbonyl} styrene (denoted as G2), and the corresponding polymers was illustrated in Scheme 1. The experimental details of the monomers' synthesis and characterization are described as follows.

### 2.3.1. Synthesis of 4-(6-bromohexyloxy) -4'-methoxy azobenzene. 4-(6-Bromohexyloxy)-4'-methoxy azobenzene was prepared according to literature [39].

$^1\text{H}$  NMR (400 MHz,  $\text{CDCl}_3$ ,  $\delta$ , ppm): 7.89–7.86 (m, 4H, Ar-H), 7.01–6.97 (m, 4H, Ar-H), 4.06–4.02 (m, 2H,  $-\text{CH}_2-$ ), 3.89 (s, 3H,  $-\text{OCH}_3$ ), 3.45–3.42 (m, 2H,  $-\text{CH}_2\text{Br}$ ), 1.93–1.82 (m, 4H,  $-\text{CH}_2-$ ), 1.55–1.51 (m, 4H,  $-\text{CH}_2-$ ).

### 2.3.2. Synthesis of Vinylterephthaloyl Chloride. An amount of 2-vinylterephthalic acid (1.92 g, 10 mmol) was mixed with thionyl chloride (20 mL) in a round-bottom flask

(100 mL). The mixture was refluxed for about 2 hr to get a clear solution. The excess thionyl chloride was removed by evaporation under reduced pressure. The residue was washed twice by petroleum ether. A pale yellow liquid of vinylterephthaloyl chloride was obtained.

### 2.3.3. Synthesis of Methyl 3, 5-di (4'-methoxy-4-oxyhexyloxy azobenzene) benzoate (**1**).

Compound **1** was obtained by the etherification of methyl 3, 5-dihydroxybenzoate with 4-(6-bromohexyloxy)-4'-methoxy azobenzene. In a three-neck round-bottom flask (1000 mL) equipped with a condenser, N<sub>2</sub> inlet–outlet, and mechanical stirrer, a mixture of K<sub>2</sub>CO<sub>3</sub> (16.56 g, 120 mmol), acetone (200 mL) was thoroughly degassed with N<sub>2</sub> for 1 hr. Methyl 3, 5-dihydroxybenzoate (3.36 g, 20 mmol) and 4-(6-bromohexyloxy)-4'-methoxy azobenzene (15.64 g, 40 mmol) were added, and the mixture was heated to 70°C. After 48 hr, the reaction was found to be complete by thin-layer chromatography (TLC). No side products were observed. The reaction mixture was filtrated. Acetone was evaporated under reduced pressure to obtain a salmon pink solid. Afterward, the crude product dissolved in dichloromethane was purified by column chromatography (silica gel, CH<sub>2</sub>Cl<sub>2</sub>). <sup>1</sup>H NMR (400 MHz, CDCl<sub>3</sub>, δ, ppm): 7.89–7.85 (m, 8H, Ar-H), 7.18–7.16 (m, 2H, Ar-H), 7.01–6.97 (m, 8H, Ar-H), 6.64–6.63 (m, 1H, Ar-H), 4.06–3.93 (m, 8H, -CH<sub>2</sub>-), 3.90 (s, 3H, -OCH<sub>3</sub>), 3.88 (s, 6H, -OCH<sub>3</sub>), 1.83–1.79 (m, 8H, -CH<sub>2</sub>-), 1.56–1.54 (m, 8H, -CH<sub>2</sub>-).

### 2.3.4. Synthesis of 3, 5-di (4'-methoxy-4-oxyhexyloxy azobenzene) benzyl alcohol (**2**).

Compound **2** was prepared by the reduction of methyl 3, 5-di (4'-methoxy-4-oxy hexyloxy azobenzene) benzoate (**1**) with LiAlH<sub>4</sub>. Compound **1** (7.88 g, 10 mmol) in dry THF (200 mL) was added slowly to a suspension of LiAlH<sub>4</sub> (0.38 g, 10 mmol) in dry THF (100 mL) at 0°C under a flow of N<sub>2</sub>. After the addition was complete, the mixture was reacted for further 2 hr at room temperature. The reaction was found to be complete by TLC. Water was then added slowly with vigorous stirring to terminate the reaction, and diluted HCl was used to adjust the pH of the mixture to 7. The product was extracted with CH<sub>2</sub>Cl<sub>2</sub>. The extracts were dried over anhydrous magnesium sulfate (anhydrous MgSO<sub>4</sub>) and condensed to give a yellow solid. Afterward, the crude product dissolved in dichloromethane was purified by column chromatography (silica gel, CH<sub>2</sub>Cl<sub>2</sub>/acetone, 50/1). <sup>1</sup>H NMR (400 MHz, CDCl<sub>3</sub>, δ, ppm): 7.90–7.86 (m, 8H, Ar-H), 7.01–6.97 (m, 8H, Ar-H), 6.52–6.51 (m, 2H, Ar-H), 6.38–6.37 (m, 1H, Ar-H), 4.62 (s, 2H, -CH<sub>2</sub>-), 4.06–3.96 (m, 8H, -CH<sub>2</sub>-), 3.88 (s, 6H, -OCH<sub>3</sub>), 1.85–1.80 (m, 8H, -CH<sub>2</sub>-), 1.56–1.55 (m, 8H, -CH<sub>2</sub>-).

### 2.3.5. Synthesis of 2, 5-bis [[3, 5-di (4'-methoxy-4-oxyhexyloxy azobenzene) benzyl] oxy-

carbonyl] styrene (Monomer G1, **3**). To a solution of **2** (15.20 g, 20 mmol), NEt<sub>3</sub> (8 mL), and DMAP (7.34 g, 60 mmol) in dried THF (100 mL) was added vinylterephthal chloride (10 mmol) at 0°C–5°C. After stirring overnight, a few drops of H<sub>2</sub>O were added to quench the reaction. The mixture was then partitioned between CH<sub>2</sub>Cl<sub>2</sub> and water. The organic layer was washed with dilute hydrochloric acid, aqueous solution of sodium bicarbonate, and brine, and dried over anhydrous MgSO<sub>4</sub> and further evaporated under reduced pressure to obtain a yellow solid. The crude product dissolved in dichloromethane was purified by column chromatography (silica gel, CH<sub>2</sub>Cl<sub>2</sub>), followed by recrystallization from THF/diethyl ether to obtain the monomer G1, **3**. <sup>1</sup>H NMR (400 MHz, CDCl<sub>3</sub>, δ, ppm): 8.29–7.95 (m, 3H, Ar-H); 7.91–7.87 (m, 16H, Ar-H), 7.49–7.42 (q, 1H, = CH-); 7.02–6.98 (m, 16H, Ar-H), 6.57 (s, 4H, Ar-H), 6.43 (s, 2H, Ar-H); 5.79–5.74 (dd, 1H, = CH<sub>2</sub>); 5.44–5.42 (dd, 1H, = CH<sub>2</sub>); 5.30, 5.28 (s, 4H, -OCH<sub>2</sub>-), 4.03–3.96 (m, 16H, -OCH<sub>2</sub>-), 3.88 (s, 12H, -OCH<sub>3</sub>),

1.87–1.83 (m, 16H, -CH<sub>2</sub>-), 1.56–1.55 (m, 16H, -CH<sub>2</sub>-). Anal. Calcd. for C<sub>100</sub>H<sub>108</sub>N<sub>8</sub>O<sub>16</sub>: C, 71.58; N, 6.68; H, 6.49; found: C, 71.41; N, 6.61; H, 6.48.

*2.3.6. Synthesis of 3, 5-di (4'-methoxy-4-oxyhexyloxy azobenzene) benzyl chloride (4).*

Compound **4** was obtained by the chlorination of **2** with SOCl<sub>2</sub>. Into a three-neck round-bottom flask (500 mL), equipped with magnetic stirrer and addition funnel, **2** (7.60 g, 10 mmol) was dissolved in dry CH<sub>2</sub>Cl<sub>2</sub> (200 mL), and a mixture of SOCl<sub>2</sub> (1.79 g, 15 mmol) and CH<sub>2</sub>Cl<sub>2</sub> (10 mL) was added dropwise slowly at room temperature. After the addition was complete, the mixture was reacted for further 2 hr at room temperature. The reaction was found to be complete by TLC. Water was then added slowly to terminate the reaction. The organic layer was washed with water, and dried over anhydrous MgSO<sub>4</sub> and further evaporated under reduced pressure to obtain a yellow solid. The crude product dissolved in dichloromethane was purified by column chromatography (silica gel, CH<sub>2</sub>Cl<sub>2</sub>). <sup>1</sup>H NMR (400 MHz, CDCl<sub>3</sub>, δ, ppm): 7.92–7.89 (m, 8H, Ar-H), 7.04–7.00 (m, 8H, Ar-H), 6.55–6.54 (m, 2H, Ar-H), 6.43–6.42 (m, 1H, Ar-H), 4.53 (s, 2H, -CH<sub>2</sub>-), 4.09–3.97 (m, 8H, -CH<sub>2</sub>-), 3.91 (s, 6H, -OCH<sub>3</sub>), 1.89–1.85 (m, 8H, -CH<sub>2</sub>-), 1.59–1.58 (m, 8H, -CH<sub>2</sub>-).

*2.3.7. Synthesis of Methyl 3, 5-di [3, 5-di (4'-methoxy-4-oxyhexyloxy azobenzene) benzyloxy] benzoate (5).*

Compound **5** was obtained by the etherification of 3, 5-dihydroxybenzoate with methyl 3, 5-di (4'-methoxy-4-oxyhexyloxy azobenzene) benzyl chloride. In a three-neck round-bottom flask (1000 mL) equipped with a condenser, N<sub>2</sub> inlet–outlet, and mechanical stirrer, a mixture of K<sub>2</sub>CO<sub>3</sub> (16.56 g, 120 mmol), acetone (200 mL) was thoroughly degassed with N<sub>2</sub> for 1 hr. Methyl 3, 5-dihydroxybenzoate (3.36 g, 20 mmol) and **4** (31.14 g, 40 mmol) were added, and the mixture was heated to 70°C. After 48 hr, the reaction was found to be complete by TLC. No side products were observed. The reaction mixture was filtrated. Acetone was evaporated under reduced pressure to obtain a salmon pink solid. Afterward, the crude product dissolved in dichloromethane was purified by column chromatography (silica gel, CH<sub>2</sub>Cl<sub>2</sub>). <sup>1</sup>H NMR (400 MHz, CDCl<sub>3</sub>, δ, ppm): 7.90–7.87 (m, 16H, Ar-H), 7.31–7.30 (m, 2H, Ar-H), 7.03–6.99 (m, 16H, Ar-H), 6.82–6.81 (m, 1H, Ar-H), 6.59–6.57 (m, 4H, Ar-H), 6.44–6.43 (m, 2H, Ar-H), 5.01 (s, 2H, -CH<sub>2</sub>-), 4.07–3.97 (m, 16H, -CH<sub>2</sub>-), 3.92 (s, 3H, -OCH<sub>3</sub>), 3.90 (s, 12H, -OCH<sub>3</sub>), 1.87–1.84 (m, 16H, -CH<sub>2</sub>-), 1.56–1.58 (m, 16H, -CH<sub>2</sub>-).

*2.3.8. Synthesis of 3, 5-di [3, 5-di (4'-methoxy-4-oxyhexyloxy azobenzene) benzyloxy] benzyl alcohol (6).*

Compound **6** was prepared by the reduction of methyl 3, 5-di [3, 5-di (4'-methoxy-4-oxyhexyloxy azobenzene) benzyloxy] benzoate with LiAlH<sub>4</sub>. Into a three-neck round-bottom flask, equipped with a condenser, ice bath, N<sub>2</sub> inlet–outlet, and magnetic stirrer, LiAlH<sub>4</sub> (0.38 g, 10 mmol) was suspended in dry THF (20 mL), and the solution of **5** (16.52 g, 10 mmol) in dry THF (200 mL) was added dropwise very slowly. After the addition was complete, the mixture was reacted for further 2 hr at room temperature. The reaction was found to be complete by TLC. Water was then added slowly to terminate the reaction, and then diluted HCl was added to dissolve the precipitate. The product was extracted with CH<sub>2</sub>Cl<sub>2</sub>. The extracts were dried over anhydrous MgSO<sub>4</sub>, and condensed to give a yellow solid. Afterward, the crude product dissolved in dichloromethane was purified by column chromatography (silica gel, CH<sub>2</sub>Cl<sub>2</sub>/acetone, 50/1). <sup>1</sup>H NMR (400 MHz, CDCl<sub>3</sub>, δ, ppm): 7.91–7.87 (m, 16H, Ar-H), 7.03–6.99 (m, 16H, Ar-H), 6.63–6.62 (m, 2H, Ar-H), 6.58–6.57 (m, 4H, Ar-H), 6.56–6.55 (m, 1H, Ar-H), 6.43–6.42 (m, 2H, Ar-H), 4.98 (s, 2H, -CH<sub>2</sub>-), 4.64 (s, 2H, -CH<sub>2</sub>-), 4.07–3.97 (m, 16H, -CH<sub>2</sub>-), 3.81 (s, 12H, -OCH<sub>3</sub>), 1.86–1.84 (m, 16H, -CH<sub>2</sub>-), 1.56–1.58 (m, 16H, -CH<sub>2</sub>-).



**2.3.9. Synthesis of 2, 5-bis {3, 5-di [3, 5-di (4'-methoxy-4-oxyhexyloxy azobenzene) benzyl] oxycarbonyl} styrene (Monomer G2, 7).** To a solution of **6** (15.20 g, 20 mmol), NEt<sub>3</sub> (8 mL), and DMAP (7.34 g, 60 mmol) in dried THF (100 mL) was added vinylterephthal chloride (10 mmol) at 0°C–5°C. After stirring overnight, a few drops of H<sub>2</sub>O were added to quench the reaction. The mixture was then partitioned between CH<sub>2</sub>Cl<sub>2</sub> and water. The organic layer was washed with dilute hydrochloric acid, aqueous solution of sodium bicarbonate, and brine, and dried over anhydrous MgSO<sub>4</sub> and further evaporated under reduced pressure to obtain a yellow solid. The crude product dissolved in dichloromethane was purified by column chromatography (silica gel, CH<sub>2</sub>Cl<sub>2</sub>), followed by recrystallization from THF/diethyl ether to obtain the monomer G2, **7**. <sup>1</sup>H NMR (400 MHz, CDCl<sub>3</sub>, δ, ppm): 8.26–8.01 (m, 3H, Ar-H); 7.97–7.94 (m, 32H, Ar-H), 7.46–7.38 (q, 1H, =CH-); 7.00–6.96 (m, 32H, Ar-H), 6.66 (s, 4H, Ar-H), 6.58 (s, 2H, Ar-H), 6.54 (s, 8H, Ar-H), 6.39 (s, 4H, Ar-H); 5.77–5.72 (dd, 1H, =CH<sub>2</sub>); 5.42–5.39 (dd, 1H, =CH<sub>2</sub>); 5.29, 5.27 (s, 4H, -OCH<sub>2</sub>-), 4.95 (s, 8H, -OCH<sub>2</sub>-), 4.01–3.93 (m, 32H, -OCH<sub>2</sub>-), 3.87 (s, 24H, -OCH<sub>3</sub>), 1.81–1.78 (m, 32H, -CH<sub>2</sub>-), 1.53–1.51 (m, 32H, -CH<sub>2</sub>-). Anal. Calcd. for C<sub>204</sub>H<sub>220</sub>N<sub>16</sub>O<sub>32</sub>: C, 71.89; N, 6.58; H, 6.51; found: C, 71.76; N, 6.53; H, 6.49.

## 2.4. Polymerization

The polymers were each obtained by conventional solution radical polymerization (see Scheme 1), typically carried out as described in the following example.

Monomer G1 (0.5 g, 0.3 mmol), 0.01 M of AIBN (150 μL) in chlorobenzene solution, and dried chlorobenzene (1.00 g) were placed in a 25 mL reaction tube with a magnetic stir bar. After three freeze-pump-thaw cycles, the tube was sealed under vacuum. Polymerization was carried out at 60°C for 24 hr. The sample was diluted with THF and precipitated into a large volume of hot acetone. The sample was purified by similarly re-precipitating three times from THF into hot acetone, and dried overnight at room temperature in vacuo.

## 3. Results and Discussion

### 3.1. Synthesis of the Monomers and the Polymers

As shown in Scheme 1, the monomers G1 and G2 were successfully synthesized through multistep reactions. The preparation and characterization of the materials, 4-(6-bromohexyloxy)-4'-methoxy azobenzene, has been described elsewhere [39]. First, methyl 3, 5-di (4'-methoxy-4-oxyhexyloxy azobenzene) benzoate was prepared by the etherification of methyl 3, 5-dihydroxybenzoate with 4-(6-bromohexyloxy)-4'-methoxy azobenzene in a hot potassium salt solution of acetone. Then, 3, 5-di (4'-methoxy-4-oxyhexyloxy azobenzene) benzyl alcohol was synthesized through the reduction between methyl 3, 5-di (4'-methoxy-4-oxyhexyloxy azobenzene) benzoate and LiAlH<sub>4</sub>. Finally, the monomer G1 was obtained by the esterification of vinylterephthaloyl chloride and 3, 5-di (4'-methoxy-4-oxyhexyloxy azobenzene) benzyl alcohol. The crude product dissolved in dichloromethane was purified by column chromatography (silica gel, CH<sub>2</sub>Cl<sub>2</sub>), followed by recrystallization from THF/diethyl ether to obtain the monomer **G1**. The synthetic protocol to prepare monomer G2 was as follows: 3, 5-di (4'-methoxy-4-oxyhexyloxy azobenzene) benzyl chloride was obtained by the chlorination of 3, 5-di (4'-methoxy-4-oxyhexyloxy azobenzene) benzyl alcohol with SOCl<sub>2</sub>. Methyl 3, 5-di [3, 5-di (4'-methoxy-4-oxyhexyloxy azobenzene) benzyloxy] benzoate was prepared by the etherification of methyl 3, 5-dihydroxybenzoate

with 3, 5-di (4'-methoxy-4-oxyhexyloxy azobenzene) benzyl chloride in a hot potassium salt solution of acetone. Then, 3, 5-di [3, 5-di (4'-methoxy-4-oxyhexyloxy azobenzene) benzyloxy] benzyl alcohol was synthesized through the reduction between methyl 3, 5-di [3, 5-di (4'-methoxy-4-oxyhexyloxy azobenzene) benzyloxy] benzoate and  $\text{LiAlH}_4$ . The last step was completed by the esterification of vinylterephthaloyl chloride and 3, 5-di [3, 5-di (4'-methoxy-4-oxyhexyloxy azobenzene) benzyloxy] benzyl alcohol. The crude product dissolved in dichloromethane was purified by column chromatography (silica gel,  $\text{CH}_2\text{Cl}_2$ ), followed by recrystallization from THF/diethyl ether to obtain the monomer **G2**. The chemical structure of the monomers **G1** and **G2** was confirmed by  $^1\text{H}$  NMR (see Fig. 1).

The polymers **PG1** were each obtained by conventional solution radical polymerization. The polymers synthesized are fusible and soluble in common organic solvents including THF, dimethylformamide (DMF), chlorobenzene, and so forth. However, it is difficult for the polymer **PG2** to obtain high MW materials because the bulky dendritic fragments inhibit the formation of polymers completely. One may speculate that the polymer **PG2** molecular resembled a capsule or a cage-like environment in which the polymerizable groups were jacketed by their own dendritic coat. As we know, due to the high mass of the dendritic monomers ( $\text{MW} = 3408$  for monomer **G2**), their molar concentration for the same weight percent concentration as of vinylterephthalic acid was 18 times lower. The increasing of concentration at the polymerization place increased dramatically the rate of polymerization and decreased initiator efficiency since the polymerizable groups were located in a very small volume fraction while the radical initiator was distributed uniformly in the reaction mixture. The high mass of monodendrons and their self-assembly forced slow their diffusion and the monodendrons were not able to migrate from their assembly to the reactive growing chain. However, the high concentration of monomer **G2** was found to be difficultly obtained in common organic solvents and be difficultly polymerized to a sufficiently high MW [13,14]. The polymers synthesized are fusible and soluble in common organic solvents including THF, DMF,  $\text{CH}_2\text{Cl}_2$ ,  $\text{CHCl}_3$ , and so forth. GPC analysis was carried out to determine the apparent MW and MW distributions of the polymers, and the molecular characterization of the polymers is summarized in Table 1.

**Table 1.** GPC, DSC, and TGA results and thermotropic properties of the polymers

Polymer <sup>a</sup>	$M_n^b (\times 10^{-4})$	$M_w/M_n^b$	$T_g$ (°C) <sup>c</sup>	Transition (°C) and corresponding enthalpy change (J/g) <sup>c</sup>	$T_d$ (N <sub>2</sub> ) (°C) <sup>d</sup>
PG1-1	2.28	1.32	48	161 (2.21)	353
PG1-2	4.27	1.57	49	162 (0.23) 184 (0.15)	356
PG1-3	5.38	1.49	48	164 (0.07) 185 (0.37)	364
PG2	2.72	1.11	45	138 (2.59)	349

<sup>a</sup>PG1 and PG2 represented the first-generation dendronized polymer and the second-generation dendronized polymer.

<sup>b</sup>Determined by GPC in THF using polystyrene standards.

<sup>c</sup>Evaluated by DSC during the second heating cycle at a rate of  $10^\circ\text{C min}^{-1}$ .

<sup>d</sup>5% weight loss temperature evaluated by TGA under a nitrogen atmosphere at a heating rate of  $20^\circ\text{C min}^{-1}$ .

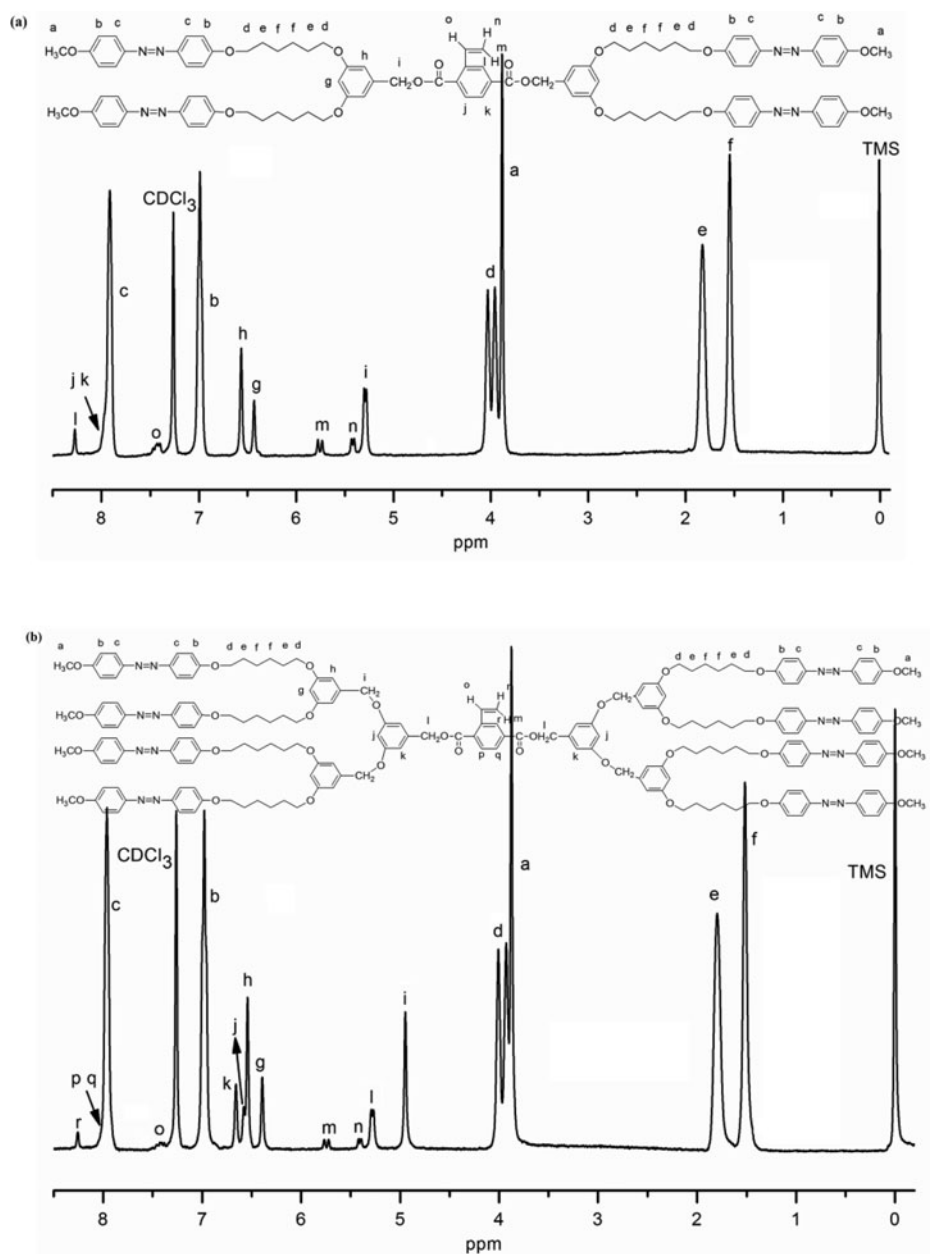


**Figure 1.**  $^1\text{H}$  NMR spectra of the monomers G1 (a) and G2 (b) in  $\text{CDCl}_3$ -d.

### 3.2. Phase Transitions and Phase Structures

TGA was employed to characterize the thermal stabilities of the polymers. As could be seen from Table 1, the polymers were quite stable, 5% weight loss occurring only above  $340^\circ\text{C}$  in nitrogen atmosphere. The phase transitions of the polymers were studied by DSC, and the transition temperatures and corresponding enthalpy changes were also summarized

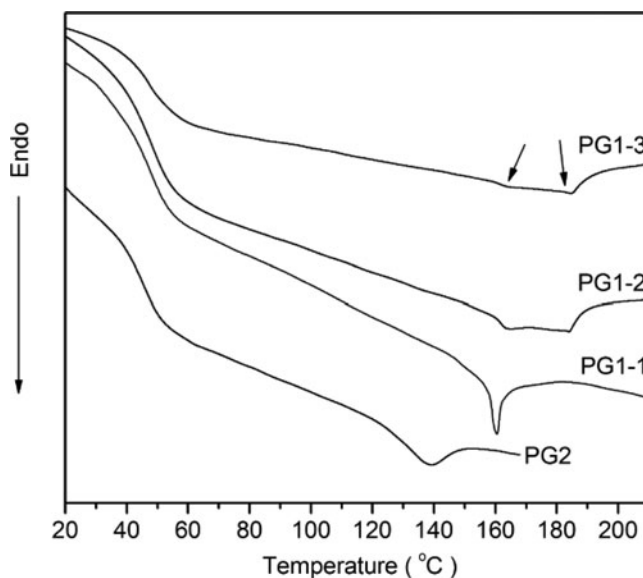


**Figure 2.** DSC curves of dendronized polymers PG1 and PG2 during the second heating at a rate of  $10^{\circ}\text{C min}^{-1}$ .

in Table 1. Figure 2 depicts a set of DSC heating traces of the three PG1 samples with different MWs and one PG2 sample recorded at a rate of  $10^{\circ}\text{C min}^{-1}$  during the second heating process. From Fig. 2 and Table 1, it will be seen that all the glass transition temperatures ( $T_g$ ) of the three PG1 samples with different MWs were  $\sim 48^{\circ}\text{C}$ , and the glass transition temperatures ( $T_g$ ) of the PG2 sample was  $\sim 45^{\circ}\text{C}$ . The  $T_g$  of the polymers decreased slightly with the generation number of the dendritic azobenzene side groups increased. The polymer PG1-1 had two phase transitions, attributed to the glass transition and the LC-isotropic phase transition, and the LC phase transition temperature ( $T_{\text{LC-I}}$ ) was  $161^{\circ}\text{C}$ . For the polymer PG1-2, careful examination revealed that two LC phase transitions were clearly observed after  $T_g$  upon heating and their LC phase transition temperatures were  $162^{\circ}\text{C}$  and  $184^{\circ}\text{C}$ , respectively. In addition, the polymer PG1-3 also had two LC phase transitions and the LC phase transition temperatures were  $164^{\circ}\text{C}$  and  $185^{\circ}\text{C}$ , respectively. However, for the polymer PG2 had only two phase transitions, attributed to the glass transition and the LC-isotropic phase transition, and the LC phase transition temperature ( $T_{\text{LC-I}}$ ) was  $138^{\circ}\text{C}$ .

The optical textures shown by the three PG1 samples with different MWs and one PG2 sample were observed using PLM. At temperature below the highest phase transition temperature ( $T_{\text{LC-I}} = 161^{\circ}\text{C}$ ), the polymer PG1-1 exhibited a representative schlieren nematic texture (see Fig. 3a), which implied that the nematic phase formed. When the sample was heated above their highest phase transition temperature, the schlieren nematic texture disappeared and isotropic phase could be observed. Both the other two PG1 samples with different MWs gave similar PLM textures. When the two samples were heated to a temperature much higher than the highest phase transition temperature, the LC birefringence was still observed and remained before decomposition. These phenomena were all similar to other MJLCPs [32,33]. Using PG1-3 as an example, Figs. 3(b)–(d) show three typical

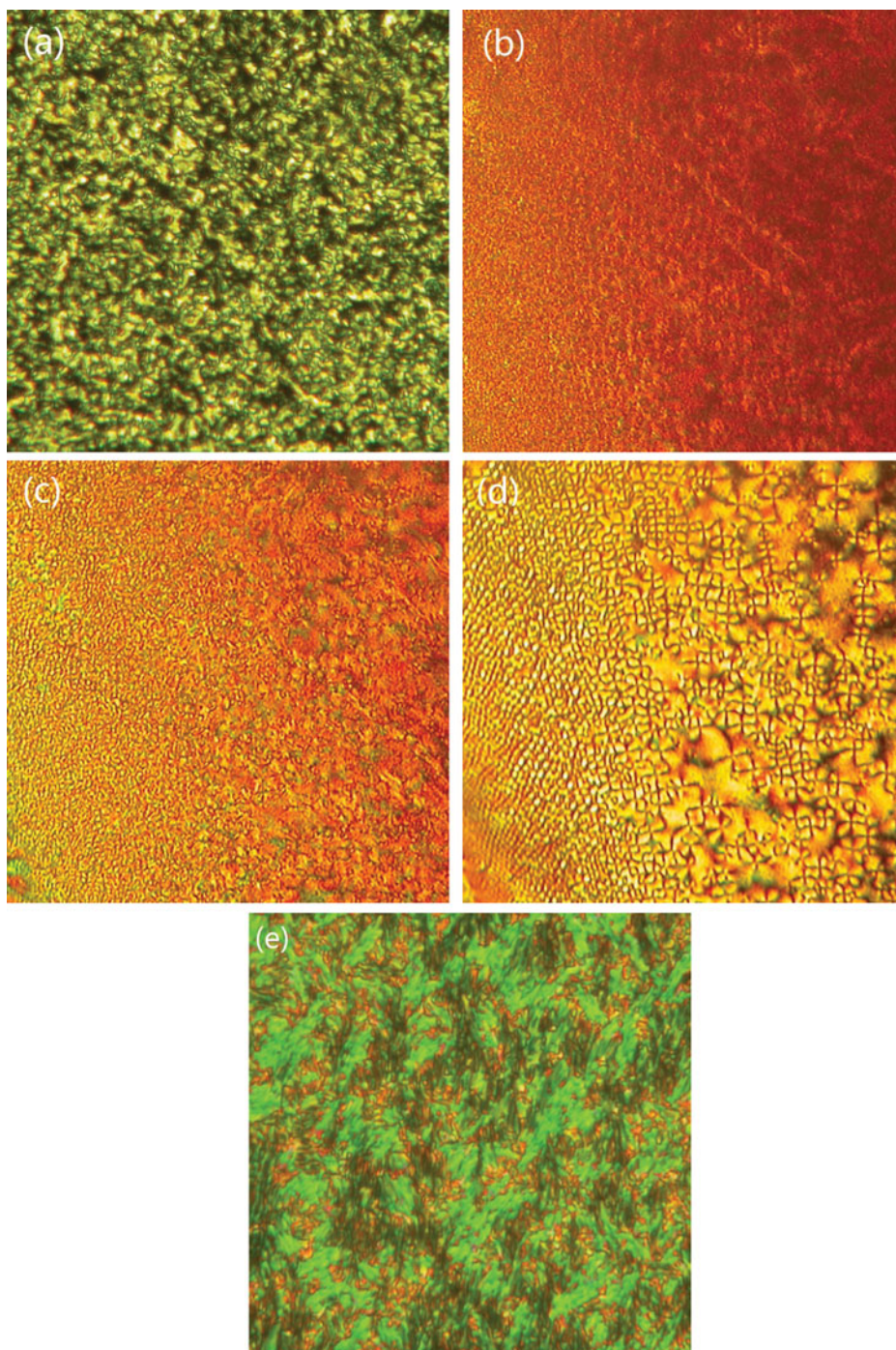


**Figure 3.** PLM images of the sample PG1-1 at (a) 150°C; the sample PG1-3 at (b) 100°C, (c) 175°C, and (d) 200°C; the sample PG2 at (e) 120°C. (Magnification:  $\times 200$ ).

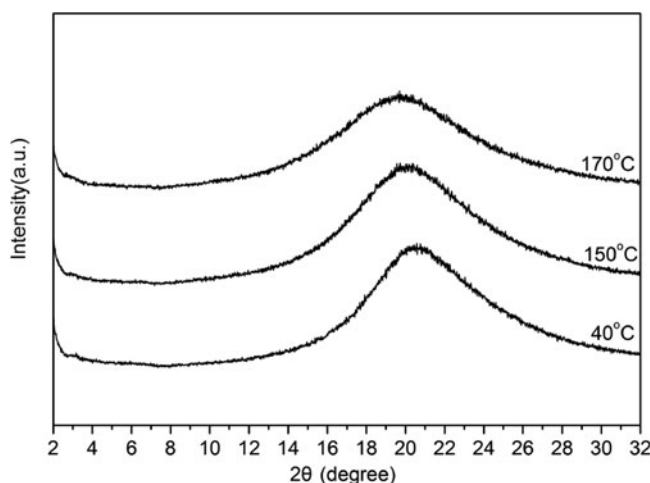


**Figure 4.** 1D WAXD patterns of the sample PG1-1 obtained during the second heating at different temperatures.

PLM images recorded at 100°C, 175°C, and 200°C, respectively, corresponding to the three LC phases. When the PG2 was heated above  $T_g$ , an obvious fan-shaped texture appeared (see Fig. 3e), indicating that the smectic phase formed. When the sample was heated above their highest phase transition temperature, however, the fan-shaped texture disappeared and isotropic phase could also be observed. Combining the DSC and PLM experimental results together, we consider that the PG1s with low MWs have one LC phase, and the PG1s with higher MWs have three LC phases and share a same phase transition sequence. For the low MW PG2, only one LC phase was observed.

To further elucidate the phase structures and transitions more clearly, 1D WAXD experiments were performed at different temperatures. Herein, the samples PG1-1, PG1-3, and PG2 will be used as the examples. Figure 4 depicts a set of 1D WAXD patterns of the polymer PG1-1 recorded during heating from 40°C to 170°C. As shown in Fig. 4, no diffraction peak can be identified in the low-angle region during the heating from 40°C to 170°C, and an intense broad peak in the high-angle region was seen below the highest phase transition temperature ( $T = 161^\circ\text{C}$ ), which indicated that only a short range order exists in the molecular lateral packing. When the sample is heated above 161°C, a typical amorphous pattern in the high-angle region is observed, implying the formation of the isotropic phase (see Fig. 4). On the basis of the results of DSC and 1D WAXD, we confirm that the LC transition of PG1-1 follows a sequence of nematic phase (N)  $\leftrightarrow$  isotropic state.

Figure 5 represents a set of 1D WAXD patterns of the polymer PG1-3 recorded during heating process. As shown in Fig. 5, five diffraction peaks at  $2.82^\circ$  ( $d$  spacing of 3.13 nm),  $3.04^\circ$  ( $d$  spacing of 2.93 nm),  $4.76^\circ$  ( $d$  spacing of 1.86 nm),  $5.06^\circ$  ( $d$  spacing of 1.75 nm), and  $5.64^\circ$  ( $d$  spacing of 1.57 nm) can be identified at 100°C, and can be assigned as (110), (200), (020), (120), and (220) diffractions of a 2D  $\Phi_R$  phase with  $a = 5.86$  nm,  $b = 3.70$  nm, and  $\gamma = 90^\circ$ . When the sample was heated above the second phase transition temperature ( $164^\circ\text{C}$ ), five diffraction peaks at  $2.70^\circ$  ( $d$  spacing of 3.27 nm),  $2.97^\circ$  ( $d$  spacing of 2.97 nm),  $4.48^\circ$  ( $d$  spacing of 1.97 nm),  $4.97^\circ$  ( $d$  spacing of 1.78 nm),

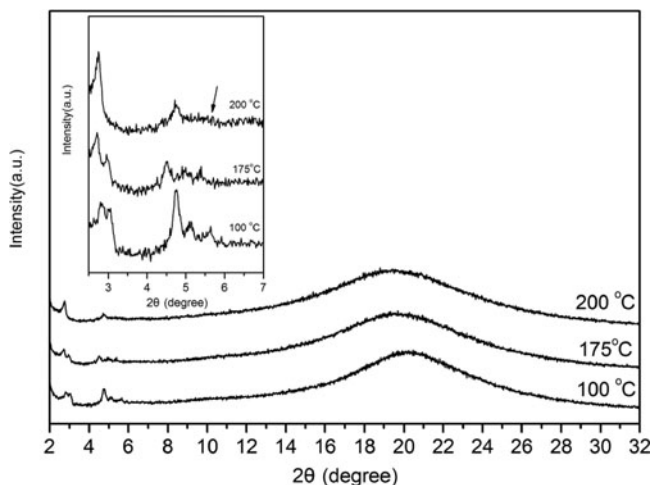


**Figure 5.** 1D WAXD patterns of the sample PG1-3 obtained during the second heating at different temperatures.

and  $5.39^\circ$  ( $d$  spacing of 1.64 nm) can be identified at  $175^\circ\text{C}$ , and can be assigned as (110), (200), (300), (310), and (220) diffractions of a 2D  $\Phi_R$  phase with  $a = 5.94$  nm,  $b = 3.92$  nm, and  $\gamma = 90^\circ$ . Notably, when the temperature overpass the third phase transition temperature ( $185^\circ\text{C}$ ), it led to a suddenly enhancement of the diffraction peak intensity at  $2.74^\circ$  ( $d$  spacing of 3.22 nm) and the peak position slightly shifted to higher  $2\theta$  angles, in addition, peak at  $2\theta = 2.97^\circ$  at  $175^\circ\text{C}$  disappears and two distinct diffraction peaks at  $4.76^\circ$  ( $d$  spacing of 1.86 nm) and  $5.49^\circ$  ( $d$  spacing of 1.61 nm) could be observed at  $200^\circ\text{C}$ . The scattering vectors of the three peaks are found to be in the ratio  $1:3^{1/2}:2$ . The three peaks can be assigned as (100), (110), and (200) diffractions, demonstrating a long-range-ordered hexagonal lattice with  $a = b = 3.22$  nm and  $\gamma = 120^\circ$ . Further heating the sample, the 2D long-range-ordered  $\Phi_H$  phase still remained before the sample decomposed. This diffraction behavior is similar to that observed from MJLCs containing two triphenylene units in the side-chains [40]. The sample renders a diffuse scattering halo at  $2\theta$  of  $\sim 20^\circ$  ( $d$  spacing of  $\sim 0.44$  nm) in the high-angle region at lower temperatures, which contributing from the packing of azobenzene-containing side-chains. When the temperature exceeds  $164^\circ\text{C}$  (the second phase transition temperature), the halo turns into a typical amorphous halo, indicating that the first LC phase transition is the melting of SmA-like structure and entering the isotropic phase.

Figure 6 depicts a set of 1D WAXD patterns of the sample PG2 recorded during heating from  $40^\circ\text{C}$  to  $150^\circ\text{C}$ . As indicated by the arrows in Fig. 6, the two diffraction peaks at  $2.94^\circ$  ( $d$  spacing of 3.00 nm) and  $4.44^\circ$  ( $d$  spacing of 1.99 nm) can be identified at  $120^\circ\text{C}$ . The scattering vectors of the two peaks are found to be in the ratio  $2:3$  and can be assigned as (200) and (300) diffractions, indicating a typical smectic phase structure. When the sample is heated above the LC phase transition temperature ( $T_{\text{LC-I}}$ ,  $138^\circ\text{C}$ ), the two peaks disappear, indicating that the sample enters an isotropic state. Combining DSC and WAXD results, it is proposed that for PG2, the LC phase transition seen is from the smectic phase to isotropic.

Combined with DSC, PLM, WAXD experiments results, we propose that the LC phase structures of the dendronized polymer containing dendritic azobenzene side groups depend

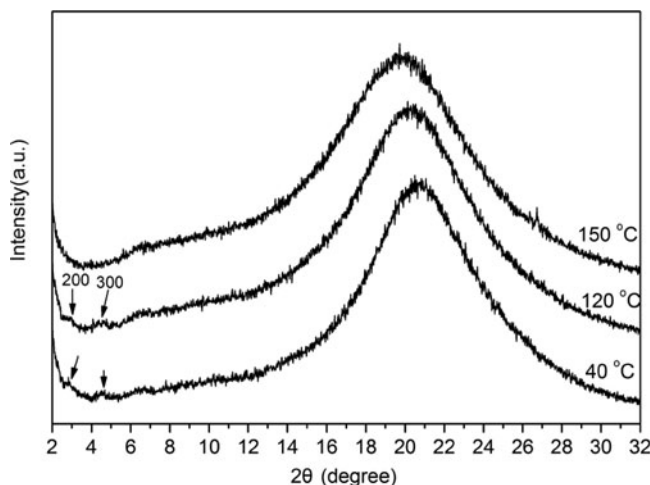


**Figure 6.** 1D WAXD patterns of the sample PG2 obtained during the second heating at different temperatures.

strongly on the MWs of polymers. For the PG1-1 with low MW, it only forms nematic phase at low temperature. Heating the polymer above the LC phase transition temperature, the isotropic state can be observed. With increasing the MWs, however, the PG1-3 can form a hierarchically ordered structure with double orderings on both the nanometer and subnanometer length scales, most likely, the thick main-chains obtained by “jacketing” the central rigid portion of side-chain to the polyethylene backbone construct a 2D centered rectangular ( $\Phi_R$ ) scaffold at lower temperature and a 2D hexagonal columnar ( $\Phi_H$ ) at higher temperature. The azobenzene-containing side-chains pack inside the main-chain scaffold form smectic A (SmA)-like structure and are perpendicular to the main-chains at lower temperature. With increasing temperature, the side-chains lose gradually the order and become isotropic state. The sequence of phase transitions of the polymer PG1-3 is followed: 2D centered rectangular  $\Phi_R$  scaffold of main-chain and SmA-like structure of side-chain  $\leftrightarrow$  2D centered rectangular  $\Phi_R$  scaffold of main-chain and isotropic side-chain  $\leftrightarrow$  2D long-range-ordered hexagonal columnar  $\Phi_H$  phase of main-chain and isotropic side-chain. Further heating the polymer, the 2D long-range-ordered  $\Phi_H$  phase of main-chain still remained before decomposed. Moreover, the generation of dendritic azobenzene side groups does also play an important role in controlling their phase behaviors and phase transitions. For the second-generation polymer PG2, it is difficult to obtain high MW materials. However, we successfully synthesized lower MW PG2, which can form an SmA-like packing. Compared the low MW PG2 with the low MW PG1-1, we found that the degree of order in LC phase increased with increasing the generation of dendritic azobenzene side groups.

#### 4. Conclusions

The first- and second-generation novel dendronized polymers containing azobenzene meso- were designed and successfully synthesized via free radical polymerization. These are poly(2, 5-bis {[3, 5-di (4'-methoxy-4-oxyhexyloxy azobenzene) benzyl] oxycarbonyl} styrene) (denoted as PG1) and poly(2, 5-bis {[3, 5-di [3, 5-di (4'-methoxy-4-oxyhexyloxy



azobenzene) benzyl] oxycarbonyl} styrene) (denoted as PG2). The chemical structure of the monomers was confirmed by elemental analysis and  $^1\text{H}$  NMR, and the corresponding polymers were studied by GPC, DSC, PLM, and 1D WAXD. The results show that the MWs and the generation of dendritic azobenzene side groups of the polymers play important roles in controlling their phase behaviors and phase transitions.

## Acknowledgment

This work is supported by the National Natural Science Foundation of China (NNSFC Grants: 21106037), the Scientific Research Fund of the Hunan Provincial Education Department (No: 11A040), and Hunan Provincial Natural Science Foundation of China (No: 12JJ4015).

## References

- [1] Tomalia, D. A., & Fréchet, J. M. J. (2002). *J. Polym. Sci. Part A: Polym. Chem.*, *40*, 2719.
- [2] Hawker, C. J., & Fréchet, J. M. J. (1992). *Polymer*, *33*, 1507.
- [3] Percec, V., Heck, J., Tomazos, D., Falkenberg, F., Blackwell, H., & Ungar, G. (1993). *J. Chem. Soc., Perkin. Trans. 1*, 2799.
- [4] Canilho, N., Kasëmi, E., Schlüter, A. D., Ruokolainen, J., & Mezzenga, R. (2007). *Macromolecules*, *40*, 7609.
- [5] Canilho, N., Kasëmi, E., Mezzenga, R., & Schlüter, A. D. (2006). *J. Am. Chem. Soc.*, *128*, 13998.
- [6] Shu, L. J., Schlüter, A. D., Ecker, C., Severin, N., & Rabe, J. P. (2001). *Angew. Chem., Int. Ed.*, *40*, 4666.
- [7] Desai, A., Atkinson, N., Rivera, F. J., Devonport, W., Rees, I., Branz, S. E., & Hawker, C. J. (2000). *J. Polym. Sci. Part A: Polym. Chem.*, *38*, 1033.
- [8] Helms, B., Mynar, J. L., Hawker, C. J., & Fréchet, J. M. J. (2004). *J. Am. Chem. Soc.*, *126*, 15020.
- [9] Tomalia, D. A., & Kirchoff, P. M. (1987). *U.S. Patent 4*, 694, 064.
- [10] Li, W., Zhang, A., Feldman, K., Walde, P., & Schlüter, A. D. (2008). *Macromolecules*, *41*, 3659.
- [11] Zhang, A., Okrasa, L., Pakula, T., & Schlüter, A. D. (2004). *J. Am. Chem. Soc.*, *126*, 6658.
- [12] Percec, V., Aqad, E., Peterca, M., Rudick, J. G., Lemon, L., Ronda, J. C., De, B. B., Heiney, P. A., & Meijer, E. W. (2006). *J. Am. Chem. Soc.*, *128*, 16365.
- [13] Percec, V., Ahn, C. H., & Barboiu, B. (1997). *J. Am. Chem. Soc.*, *119*, 12978.
- [14] Percec, V., Ahn, C. H., Ungar, G., Yeardley, D. J. P., Moller, M., & Sheiko, S. S. (1998). *Nature*, *391*, 161.
- [15] Percec, V., Imam, M. R., Peterca, M., Wilson, D. A., Graf, R., Spiess, H. W., Balagurusamy, V. S. K., & Heiney, P. A. (2009). *J. Am. Chem. Soc.*, *131*, 7662.
- [16] Rosen, B. M., Wilson, C. J., Wilson, D. A., Peterca, M., Imam, M. R., & Percec, V. (2009). *Chem. Rev.*, *109*, 6275.
- [17] Percec, V., Hudson, S. D., Peterca, M., Leowanawat, P., Aqad, E., Graf, R., Spiess, H. W., Zeng, X. B., Ungar, G., & Heiney, P. A. (2011). *J. Am. Chem. Soc.*, *133*, 18479.
- [18] Percec, V., Peterca, M., Tadjiev, T., Zeng, X. B., Ungar, G., Leowanawat, P., Aqad, E., Imam, M. R., Rosen, B. M., Akbey, U., Graf, R., Sekharan, S., Sebastiani, D., Spiess, H. W., Heiney, P. A., & Hudson, S. D. (2011). *J. Am. Chem. Soc.*, *133*, 12197.
- [19] Percec, V., Imam, M. R., Peterca, M., & Leowanawat, P. (2012). *J. Am. Chem. Soc.*, *134*, 4408.
- [20] Percec, V., Sun, H. J., Leowanawat, P., Peterca, M., Graf, R., Spiess, H. W., Zeng, X. B., Ungar, G., & Heiney, P. A. (2013). *J. Am. Chem. Soc.*, *135*, 4129.
- [21] Chen, Y. M., Chen, C. F., Liu, W. H., Li, Y. F., & Xi, F. (1996). *Macromol. Rapid. Commun.*, *17*, 401.
- [22] Jiao, Q., Yi, Z., Chen, Y. M., & Xi, F. (2008). *J. Polym. Sci. Part A: Polym. Chem.*, *46*, 4564.

- [23] Xiong, X. Q., Chen, Y. M., Feng, S., & Wang, W. (2007). *Macromolecules*, 40, 9084.
- [24] Al-Hellani, R., & Schlüter, A. D. (2006). *Macromolecules*, 39, 8943.
- [25] Hietala, S., Nyström, A. M., Tenhu, H., & Hult, A. (2006). *J. Polym. Sci. Part A: Polym. Chem.*, 44, 3674.
- [26] Zhou, Q. F., Li, H. M., & Feng, X. D. (1987). *Macromolecules*, 20, 233.
- [27] Zhou, Q. F., Zhu, X. L., & Wen, Z. Q. (1989). *Macromolecules*, 22, 491.
- [28] Tu, Y. F., Wan, X. H., Zhang, D., Zhou, Q. F., & Wu, C. (2000). *J. Am. Chem. Soc.*, 122, 10201.
- [29] Yin, X. Y., Ye, C., Ma, X., Chen, E. Q., Qi, X. Y., Duan, X. F., Wan, X. H., Cheng, S. Z. D., & Zhou, Q. F. (2003). *J. Am. Chem. Soc.*, 125, 6854.
- [30] Tu, Y. F., Wan, X. H., Zhang, H. L., Fan, X. H., Chen, X. F., Zhou, Q. F., & Chau, K. (2003). *Macromolecules*, 36, 6565.
- [31] Li, C. Y., Tenneti, K. K., Zhang, D., Zhang, H. L., Wan, X. H., Chen, E. Q., & Zhou, Q. F. (2004). *Macromolecules*, 37, 2854.
- [32] Ye, C., Zhang, H. L., Huang, Y., Chen, E. Q., Lu, Y. L., Shen, D. Y., Wan, X. H., Shen, Z. H., Cheng, S. Z. D., & Zhou, Q. F. (2004). *Macromolecules*, 37, 7188.
- [33] Chen, X. F., Tenneti, K. K., Li, C. Y., Bai, Y. W., Zhou, R., Wan, X. H., Fan, X. H., & Zhou, Q. F. (2006). *Macromolecules*, 39, 517.
- [34] Jin, H., Xu, Y. D., Shen, Z. H., Zou, D. C., Wang, D., Zhang, W., Fan, X. H., & Zhou, Q. F. (2010). *Macromolecules*, 43, 8468.
- [35] Jones, C., & Day, S. (1991). *Nature*, 351, 15.
- [36] Yu, Y. L., Nakano, M., & Ikeda, T. (2003). *Nature*, 425, 145.
- [37] Tian, Y., Watanabe, K., Kong, X., Abe, J., & Iyoda, T. (2002). *Macromolecules*, 35, 3739.
- [38] Liu, Y. X., Zhang, D., Wan, X. H., & Zhou, Q. F. (1998). *Chin. J. Polym. Sci.*, 16, 283.
- [39] Stewart, D., & Imrie, C. T. (1996). *Polymer*, 37, 3419.
- [40] Zhu, Y. F., Guan, X. L., Shen, Z. H., Fan, X. H., & Zhou, Q. F. (2012). *Macromolecules*, 45, 3346.